Millisecond Exposures in Ground-Based Exoplanet Imaging

Richard A. Frazin

University of Michigan

Fundamental Problems with Differential Imaging

It does not work within ≈ 3 λ/D of the star

But that is the most productive part of the image!

- Not enough diurnal rotation
- Statistical Penalty (Mawet et al.)
- Way to close to center for SDI to help

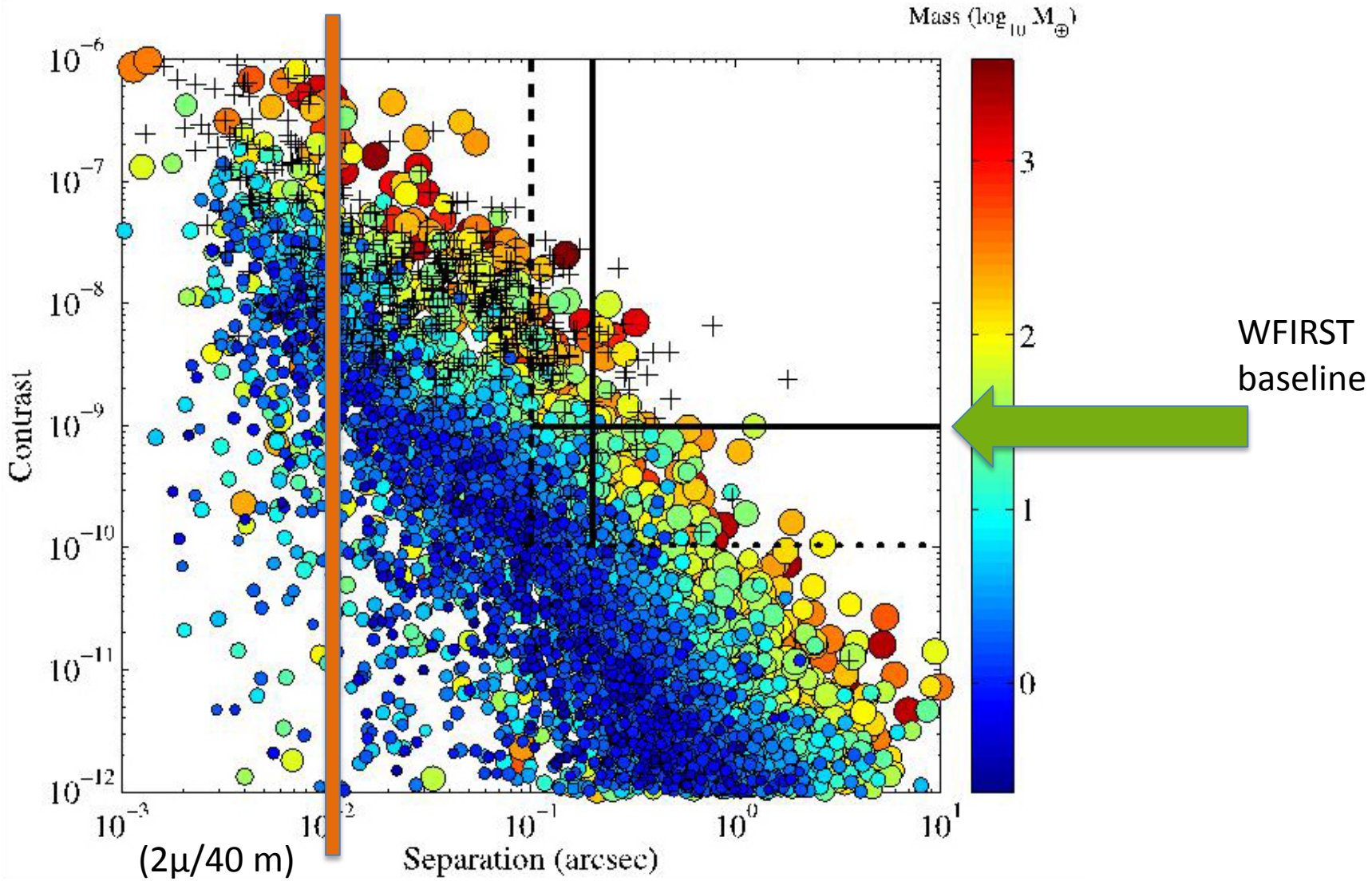

Contrast vs. Separation. Colored circles show a simulation of model planets, ranging in size from Mars-like to several times the radius of Jupiter, placed in orbit around ~200 of the nearest stars within 30 pc. The model assumes roughly four planets per star with a mixture of gas giants, ice giants, and rocky planets, and a size and radius distribution consistent with Kepler results. Color indicates planet mass while size indicates planet radius. Crosses represent known radial velocity planets at their maximum possible contrast values. (WFIRST website)

The Astrophysical Journal, 795:122 (20pp), 2014 November 10 doi:10.1088/0004-637X/795/2/

MAXIMIZING THE ExoEarth CANDIDATE YIELD FROM A FUTURE DIRECT IMAGING MISSION

Christopher C. Stark[1], Aki Roberge[2], Avi Mandell[2], and Tyler D. Robinson[3]
[1] NASA Goddard Space Flight Center, Exoplanets & Stellar Astrophysics Laboratory, Code 667, Greenbelt, MD 20771, USA; christopher.c.stark@nasa.gov
[2] NASA Goddard Space Flight Center, Greenbelt, MD 20771, USA
[3] NASA Ames Research Center, Moffett Field, CA 94035, USA
Received 2014 May 20; accepted 2014 September 17; published 2014 October 21

ABSTRACT

ExoEarth yield is a critical science metric for future exoplanet imaging missions. Here we estimate exoEarth candidate yield using single visit completeness for a variety of mission design and astrophysical parameters. We review the methods used in previous yield calculations and show that the method choice can significantly impact yield estimates as well as how the yield responds to mission parameters. We introduce a method, called Altruistic Yield Optimization, that optimizes the target list and exposure times to maximize mission yield, adapts maximally to changes in mission parameters, and increases exoEarth candidate yield by up to 100% compared to previous methods. We use Altruistic Yield Optimization to estimate exoEarth candidate yield for a large suite of mission and astrophysical parameters using single visit completeness. We find that exoEarth candidate yield is most sensitive to telescope diameter, followed by coronagraph inner working angle, followed by coronagraph contrast, and finally coronagraph contrast noise floor. We find a surprisingly weak dependence of exoEarth candidate yield on exozodi level. Additionally, we provide a quantitative approach to defining a yield goal for future exoEarth-imaging missions.

The Astrophysical Journal, 799:87 (10pp), 2015 January 20 doi:10.1088/0004-637X/799/1/87

SCIENCE PARAMETRICS FOR MISSIONS TO SEARCH FOR EARTH-LIKE EXOPLANETS BY DIRECT IMAGING

Robert A. Brown
Space Telescope Science Institute, 3700 San Martin Drive, Baltimore, MD 21218, USA; rbrown@stsci.edu
Received 2014 February 7; accepted 2014 November 11; published 2015 January 19

ABSTRACT

We use N_t, the number of exoplanets observed in time t, as a science metric to study direct-search missions like *Terrestrial Planet Finder*. In our model, N has 27 parameters, divided into three categories: 2 astronomical, 7 instrumental, and 18 science-operational. For various "27-vectors" of those parameters chosen to explore parameter space, we compute design reference missions to estimate N_t. Our treatment includes the recovery of completeness c after a search observation, for revisits, solar and antisolar avoidance, observational overhead, and follow-on spectroscopy. Our baseline 27-vector has aperture $D = 16$ m, inner working angle IWA $= 0.039''$, mission time $t = 0$–5 yr, occurrence probability for Earth-like exoplanets $\eta = 0.2$, and typical values for the remaining 23 parameters. For the baseline case, a typical five-year design reference mission has an input catalog of ~4700 stars with nonzero completeness, ~1300 unique stars observed in ~2600 observations, of which ~1300 are revisits, and it produces $N_1 \sim 50$ exoplanets after one year and $N_5 \sim 130$ after five years. We explore offsets from the baseline for 10 parameters. We find that N depends strongly on IWA and only weakly on D. It also depends only weakly on zodiacal light for $Z < 50$ zodis, end-to-end efficiency for $h > 0.2$, and scattered starlight for $\zeta < 10^{-10}$. We find that observational overheads, completeness recovery and revisits, solar and antisolar avoidance, and follow-on spectroscopy are all important factors in estimating N.

The Astrophysical Journal, 792:97 (11pp), 2014 September 10 doi:10.1088/0004-637X/792/2/97

FUNDAMENTAL LIMITATIONS OF HIGH CONTRAST IMAGING SET BY SMALL SAMPLE STATISTICS

D. Mawet[1], J. Milli[1], Z. Wahhaj[1], D. Pelat[2], O. Absil[3,10], C. Delacroix[3], A. Boccaletti[4], M. Kasper[5], M. Kenworthy[6], C. Marois[7], B. Mennesson[8], and L. Pueyo[9]

[1] European Southern Observatory, Alonso de Cordóva 3107, Vitacura, Santiago, Chile
[2] LUTH, Observatoire de Paris, CNRS, UPMC and University Paris Diderot, 5 place Jules Janssen, F-92195 Meudon, France
[3] Département d'Astrophysique, Géophysique et Océanographie, Université de Liège, 17 Allée du Six Août, B-4000 Liège, Belgium
[4] LESIA, Observatoire de Paris, CNRS, UPMC and University Paris Diderot, 5 place Jules Janssen, F-92195 Meudon, France
[5] European Southern Observatory Headquarters, Karl-Schwarzschild-Strasse 2, D-85748 Garching bei München, Germany
[6] Leiden Observatory, Leiden University, P.O. Box 9513, 2300-RA Leiden, The Netherlands
[7] NRC, Herzberg Institute of Astrophysics, Victoria, BC V9E 2E7, Canada
[8] Jet Propulsion Laboratory, California Institute of Technology, 4800 Oak Grove Drive, Pasadena, CA 91109, USA
[9] Space Telescope Science Institute, 3700 San Martin Drive, Baltimore, MD 21218, USA
Received 2014 January 16; accepted 2014 July 7; published 2014 August 21

ABSTRACT

In this paper, we review the impact of small sample statistics on detection thresholds and corresponding confidence levels (CLs) in high-contrast imaging at small angles. When looking close to the star, the number of resolution elements decreases rapidly toward small angles. This reduction of the number of degrees of freedom dramatically affects CLs and false alarm probabilities. Naively using the same ideal hypothesis and methods as for larger separations, which are well understood and commonly assume Gaussian noise, can yield up to one order of magnitude error in contrast estimations at fixed CL. The statistical penalty exponentially increases toward very small inner working angles. Even at 5–10 resolution elements from the star, false alarm probabilities can be significantly higher than expected. Here we present a rigorous statistical analysis that ensures robustness of the CL, but also imposes a substantial limitation on corresponding achievable detection limits (thus contrast) at small angles. This unavoidable fundamental statistical effect has a significant impact on current coronagraphic and future high-contrast imagers. Finally, the paper concludes with practical recommendations to account for small number statistics when computing the sensitivity to companions at small angles and when exploiting the results of direct imaging planet surveys.

Key words: methods: statistical – techniques: high angular resolution

Online-only material: color figures

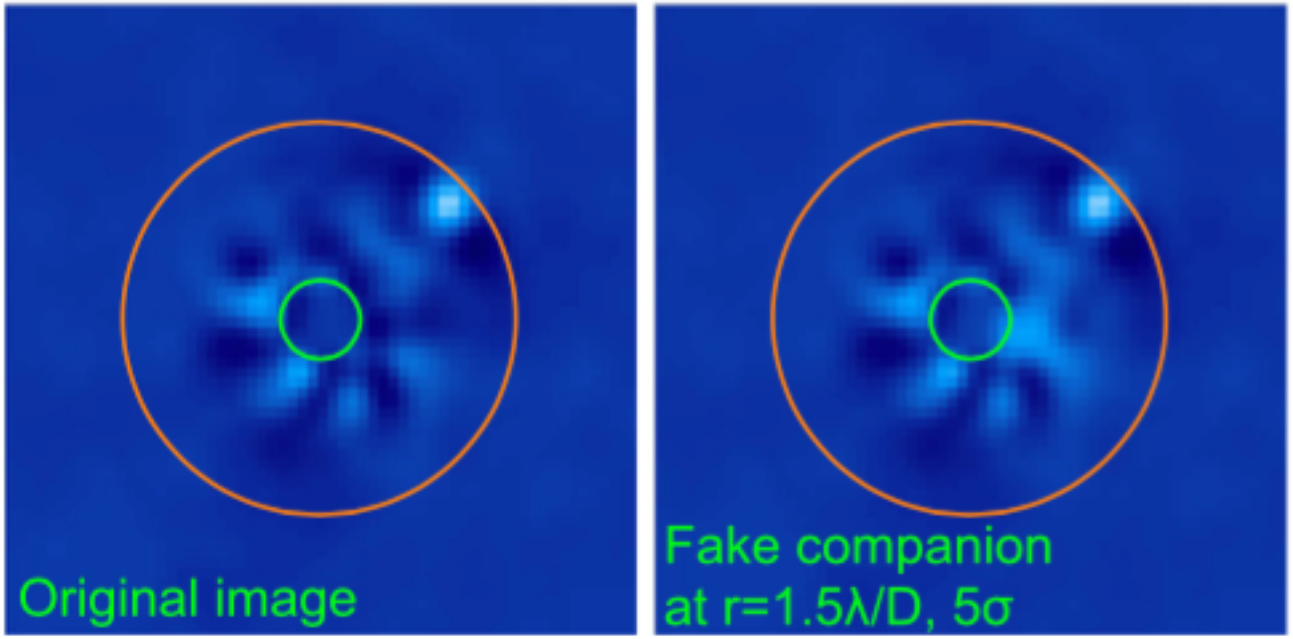

Figure 3. β Pictoris contrast curve (top, continuous curve) and image (bottom left, north is not up) taken with NACO in the L band (Absil et al. 2013), both corrected for the ADI-PCA data reduction throughput. The small green circle is of radius $r = 1\lambda/D$, while the big orange circle is of radius $r = 5\lambda/D$. A fake planet was injected at $r = 1.5\lambda/D$ (to the right of the green circle) at the 5σ throughput-corrected contrast level as presented in Absil et al. (2013). This 5σ fake companion is supposedly yielding a solid detection, rejecting the null hypothesis at the $1\text{–}3 \times 10^{-7}$ CL, assuming normally distributed noise. This is clearly not the case here because of the effect of small sample statistics at small angles. The FPF curve (dashed line) traces the increase of false alarm probability (or equivalently, the decrease of CL) toward small angles. Note that the scale of the y axis is unique, the contrast and FPF curves being dimensionless. Both quantities are related but have different meanings (see the text for details).

Mawet et al. (2014)

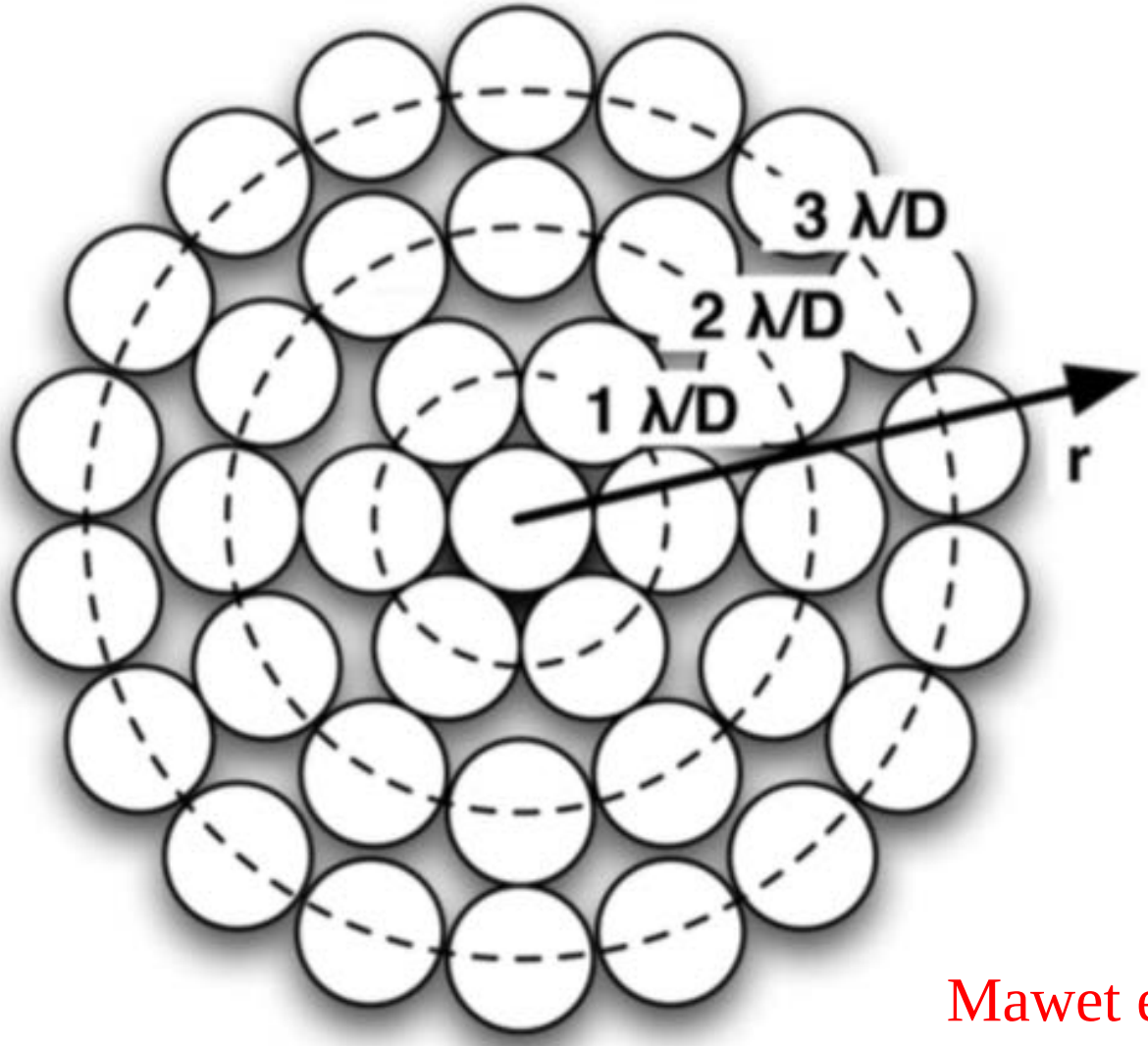

Mawet et al. (2014)

Figure 4. Number of resolution elements at a given radius r, is $2\pi r$ (here shown for r ranging from 1 to 3 λ/D). At close separation, the speckle PDF nature is likely varying drastically as a function of r because of the well-known sensitivity of the PSF to low-order aberrations, especially after a coronagraph.

more ADI problems

- ADI implicitly assumes that the aberrations are not evolving during the course of the observing period (hours, days, or more). But, due to varying mechanical and thermal stress, they are.
- ADI will remove any feature with circular symmetry, whether or not it part of the image. Thus, it is not true imaging.
- Self-subtraction is very problematic since the most informative images are the closest in time and have the least diurnal rotation.

β pic results from MagAO Clio, ADI (KLIP) processing. (Morzinski et al. 2015)

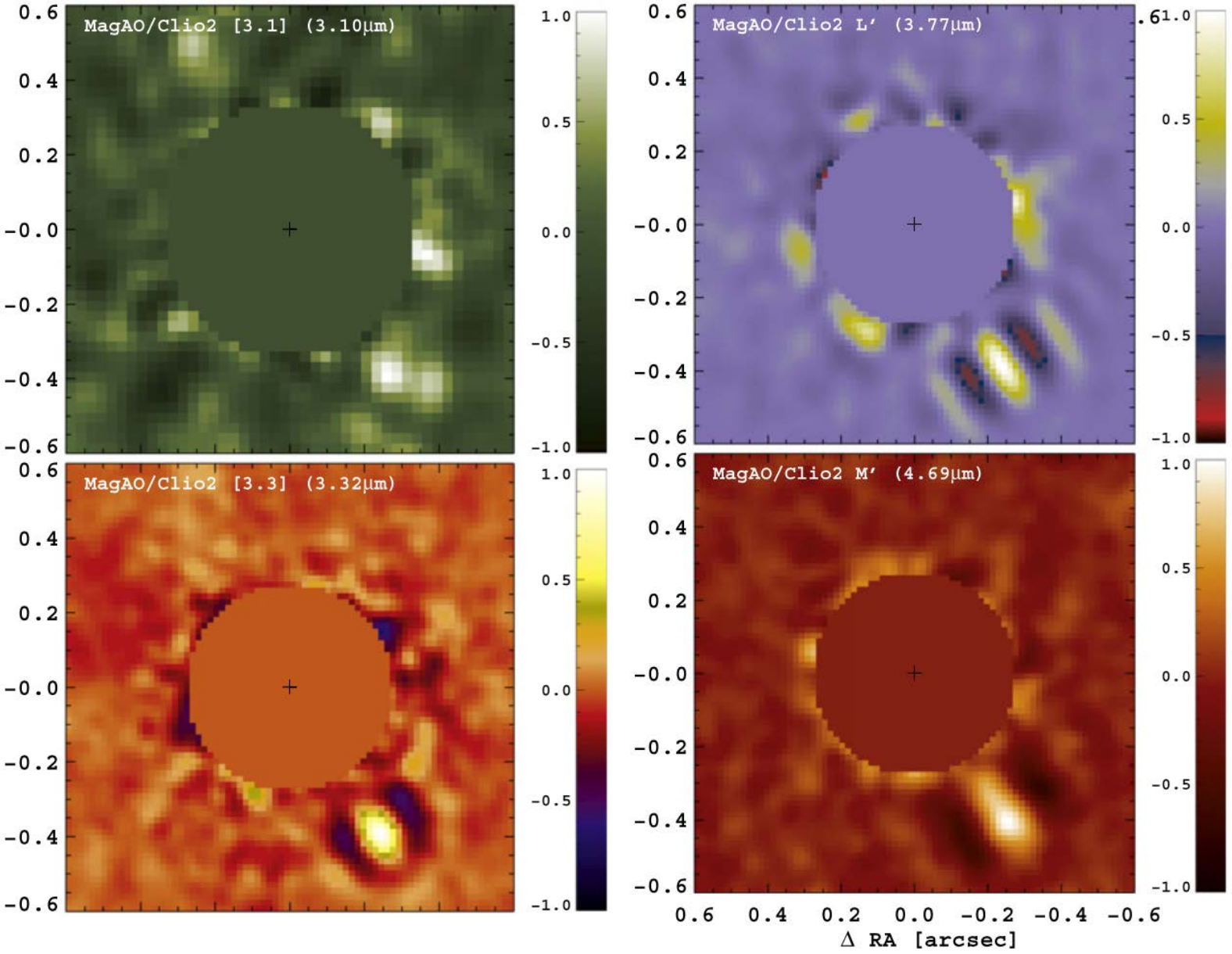

ADI problems, cont'd.

- Wind characteristics change over time, resulting in a turbulent PSF that changes
- Any pointing jitter changes PSF with coronagraph (unless the coronagraph is pupil plane only)
- Speckle cancellation/"dark hole" methods won't work nearly as well in space (more later)
- Arbitrary parameters in ADI processing

HD106906 pic results from GPI, ADI (KLIP) processing.
Kalas et al. 2015)

standard KLIP
Stokes I

interpolated KLIP
Stokes I

standard KLIP
Stokes Qr

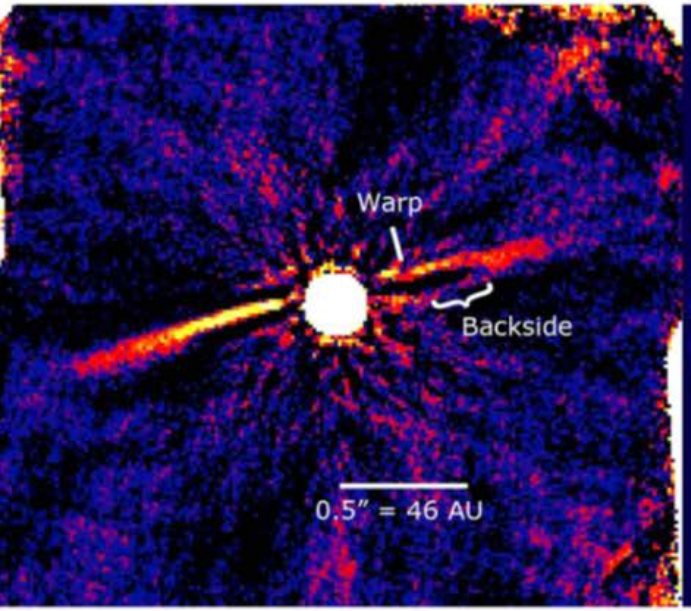

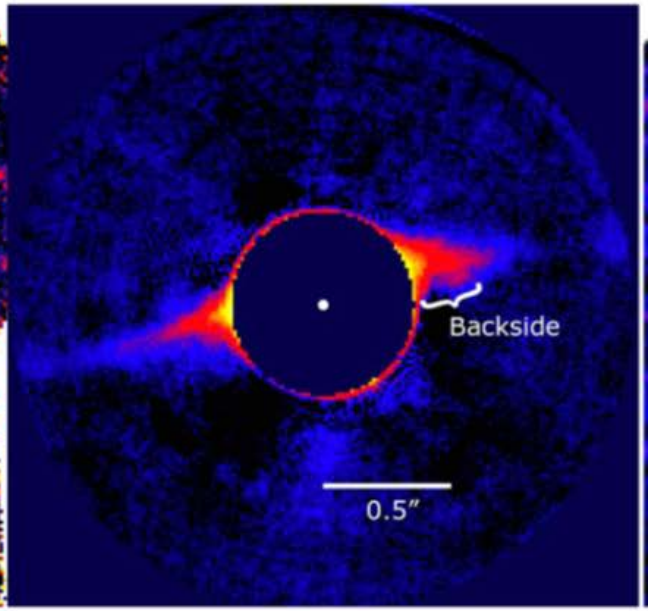

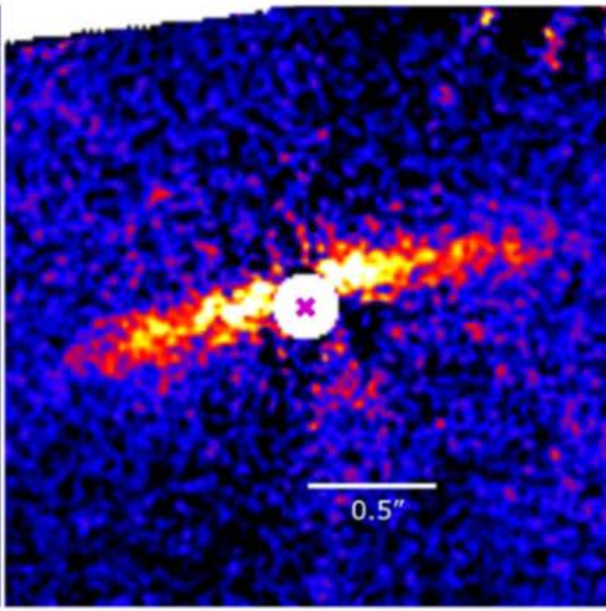

self-subtraction
evident

self-subtraction
mitigated

Q: Then, What Can Be Done?

A: Take millisecond data in the science camera in sync with the WFS → comprehensive statistical inference solution to estimate aberrations and planetary image simultaneously

Why?

ms imaging + statistical inference leaves no information on the table

- takes advantage of millisecond information not available in exposures that average over the turbulence → can work near IWA of coronagraph (no Mawet statistical penalty)
- can utilize constraints from diurnal rotation (as ADI does)
- can utilize multi-wavelength constraints (as SDI does
- point-source assumption not necessary (but can be used)

Information Content of Millisecond Exposures in Ground-Based Exoplanet Imaging

ms exposures and self-coherent cameras are the only things that can find planets within $\approx 3\ \lambda/D$ of the star because differential imaging does not.

Least controversial motivation to study millisecond focal plane sensing:

SELEX and MKIDS near-IR detectors!

Capable of kHz readout rates and have sub-electron read noise. Need to explore how they can be applied.

What happens on ms time-scales?

- At the center of a planet's Airy disk, the AO system holds its intensity nearly constant (unless near IWA)
- At the center of a planet's Airy disk, the stellar intensity is fluctuating wildly.
- The ms fluctuations of the speckle light encode information about the aberrations, carrying a tremendous amount of information about them
- This information is readily (maybe not so readily…) available since the residual phase is measured by the WFS.

Illustration of Available Info: Vibration Detection with FP Sensing

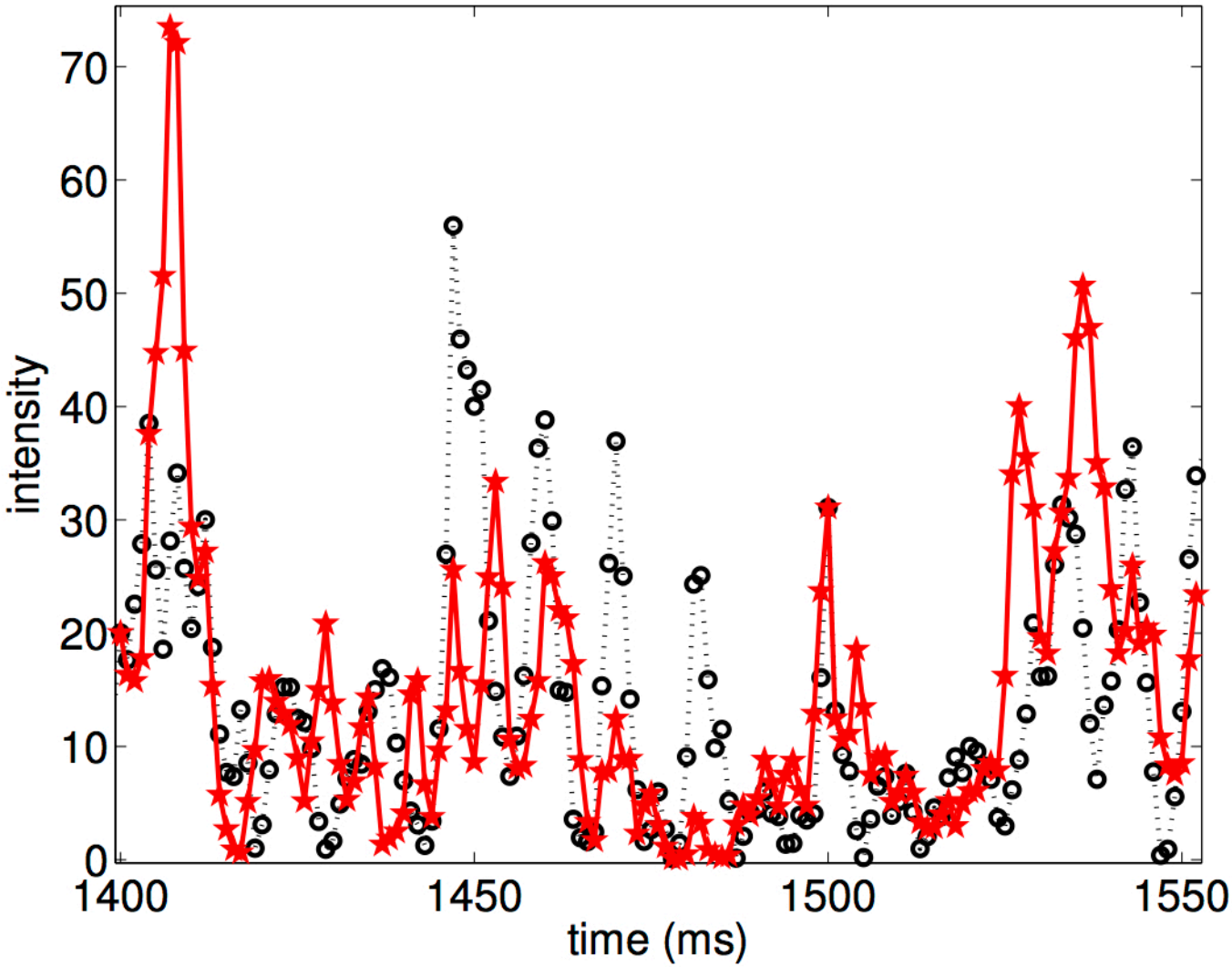

Frazin, SPIE 2014

- Turbulent modulation of speckle caused high frequency vibrations. Red: 10 Hz Black: 100 Hz.

My Coronagraph Simulations

- I started with a series of 4000 measured wavefronts from the AEOS AO system (thanks to Lewis Roberts at JPL)
- Then I simulated how a simple stellar coronagraph would respond to these wavefronts
- I included “unknown” aberration in the optical system, including a sinusoidal term with a spatial frequency that placed a speckle exactly over the simulated planet.

Aberration (pupil plane)

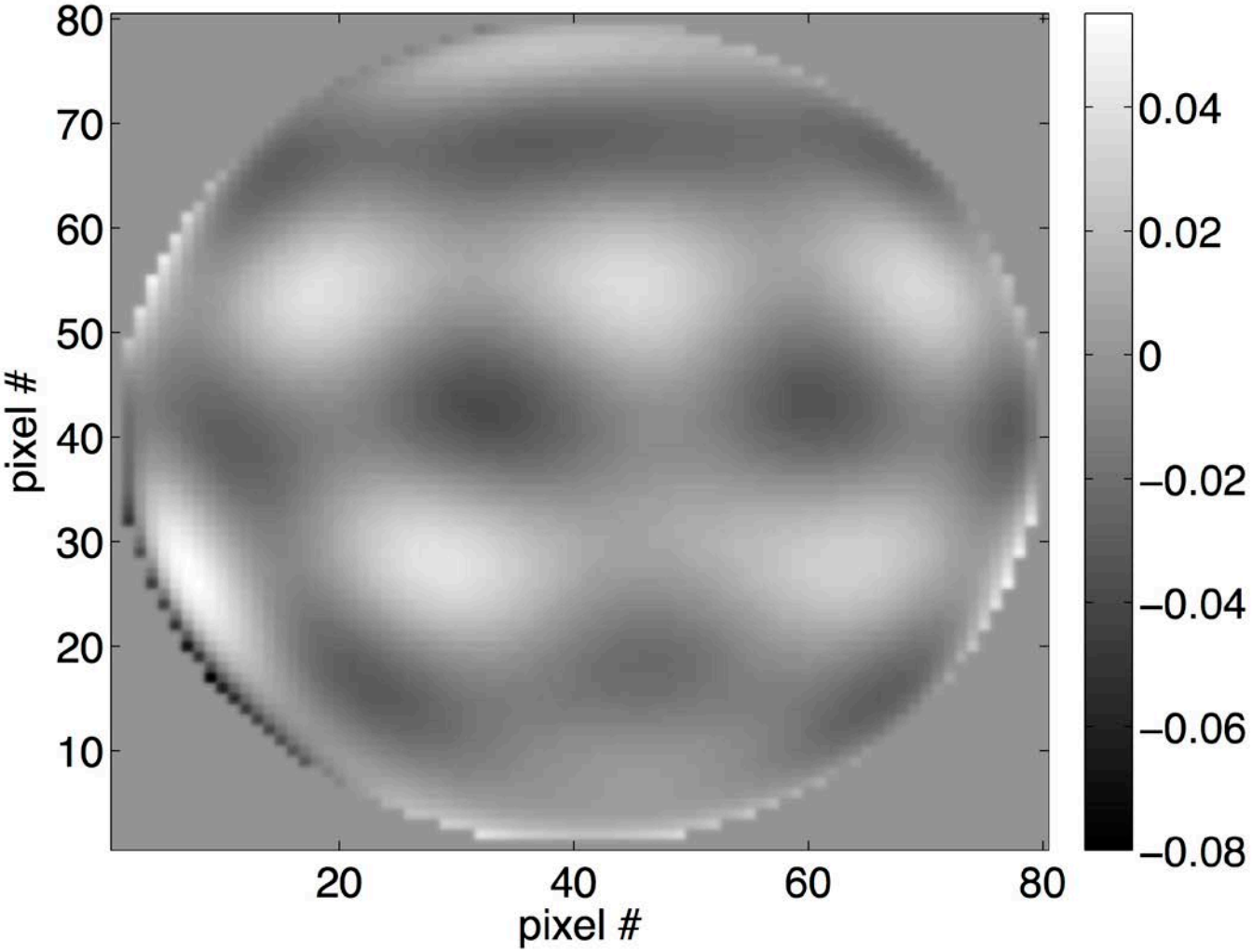

Aberration used in simulation (sinusoid + Zernicke polynomials).

Image of Star w/ Aberration

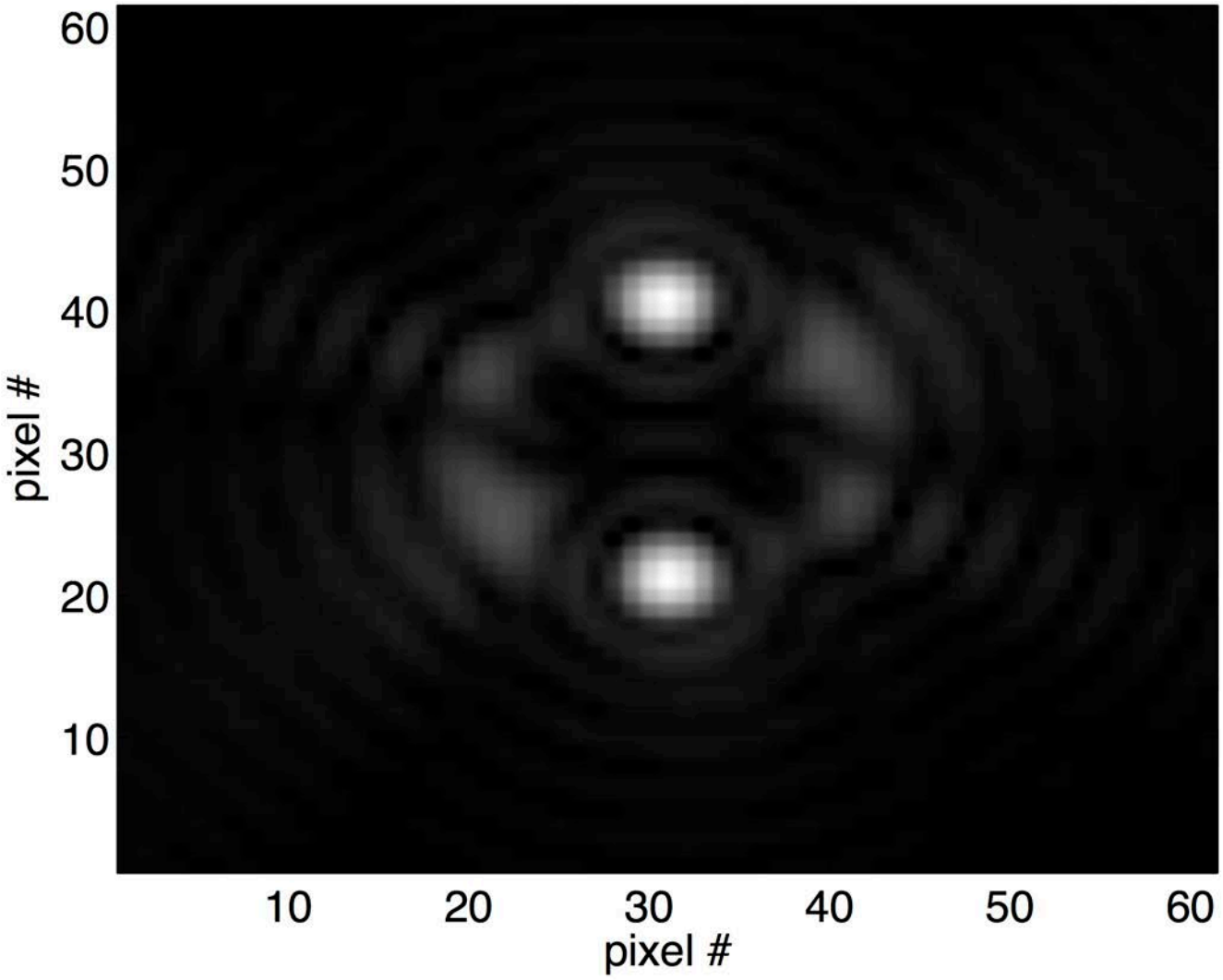

Image plane manifestation of aberration used in simulation (flat wavefront). One of the dots is exactly coincident with a planet.

Coronagraph (Companion 1%)

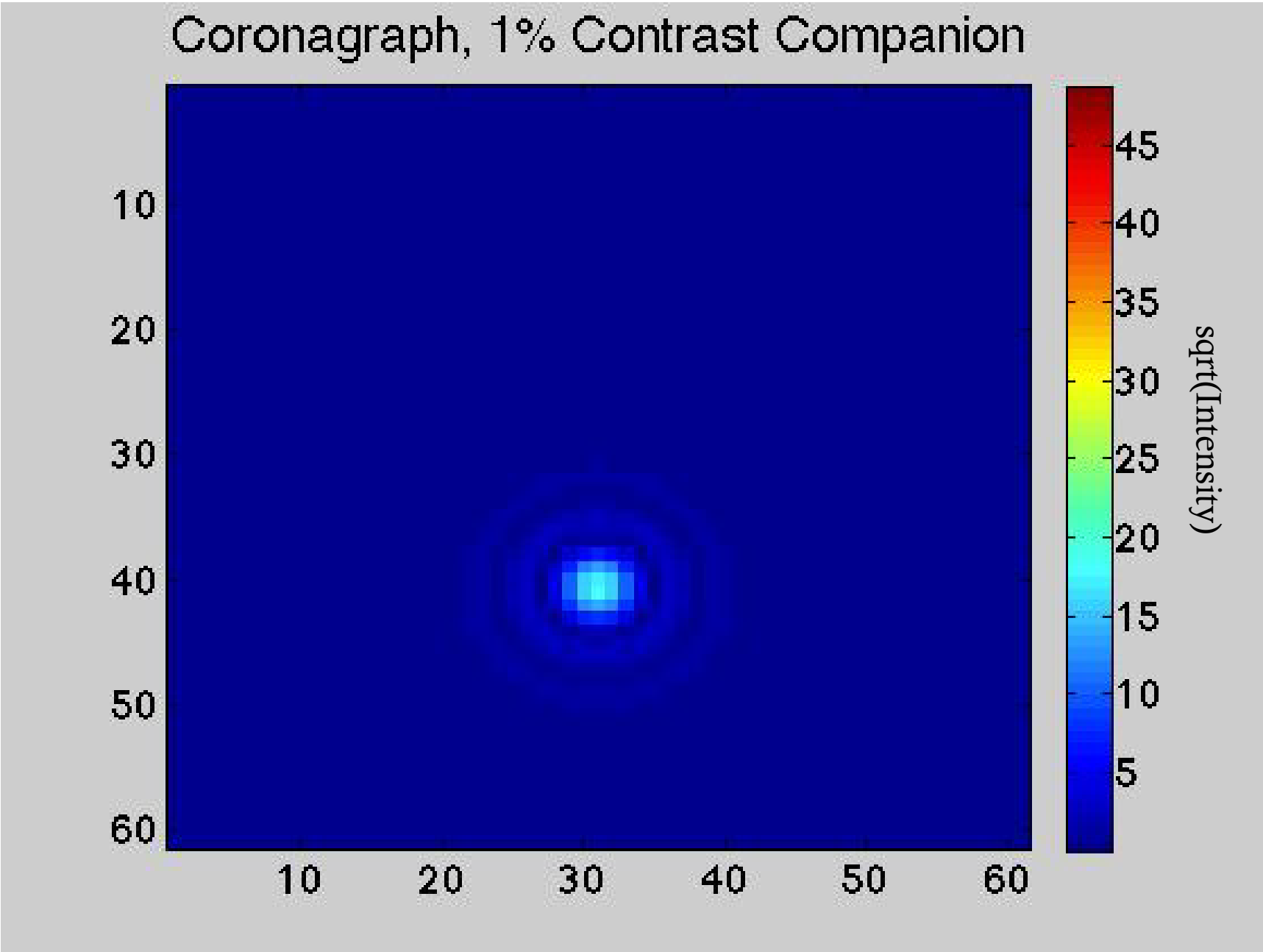

Coronagraph Simulations

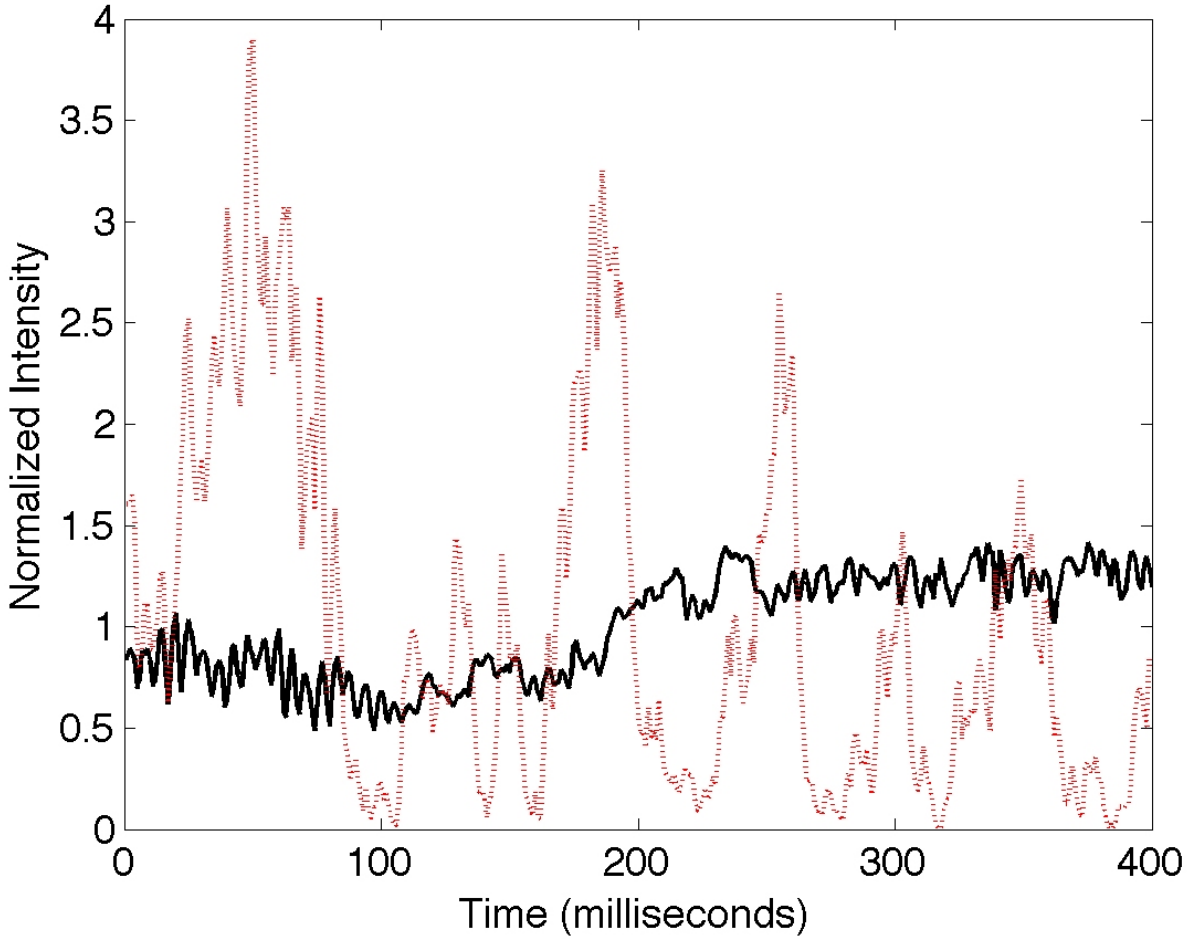

Red: stellar speckle intensity (normalized at planet position. Black: Planet intensity (normalized) at same position.

I demonstrated this effect analytically using physical optics arguments in my 2013 ApJ.

Q: How do you use the ms information?

A: 2 methods:

- “statistical deconvolution” (treat as histogram)
- comprehensive regression approach (treat as time-series)

“statistical deconvolution”

Statistics of intensity in adaptive-optics images and their usefulness for detection and photometry of exoplanets

Szymon Gladysz,[1,*] Natalia Yaitskova,[1] and Julian C. Christou[2]

[1]*European Organization for Astronomical Research in the Southern Hemisphere (ESO), Karl Schwarzschildstrasse 2, D-85748 Garching B. Muenchen, Germany*
[2]*Gemini Observatory, 670 North A'ohoku Place, Hilo, Hawaii 96720, USA*
[*]*Corresponding author: sgladysz@eso.org*

Received April 14, 2010; accepted May 28, 2010;
posted June 18, 2010 (Doc. ID 127027); published August 5, 2010

This paper is an introduction to the problem of modeling the probability density function of adaptive-optics speckle. We show that with the modified Rician distribution one cannot describe the statistics of light on axis. A dual solution is proposed: the modified Rician distribution for off-axis speckle and gamma-based distribution for the core of the point spread function. From these two distributions we derive optimal statistical discriminators between real sources and quasi-static speckles. In the second part of the paper the morphological difference between the two probability density functions is used to constrain a one-dimensional, “blind,” iterative deconvolution at the position of an exoplanet. Separation of the probability density functions of signal and speckle yields accurate differential photometry in our simulations of the SPHERE planet finder instrument.

OCIS codes: 010.1080, 030.6140, 030.6600, 030.7060, 350.1270, 100.2980.

“statistical deconvolution” idea: histogram fitting

- Histogram of stellar speckle intensity at any pixel is given by modified Rician distribution - 2 free params
- At planet position, histogram of planet intensity is given by histogram of Strehl ratio (Maréchal approx.) – 1 free param
- Fit 2 histograms to get planet intensity and modified Rician parameters

“statistical deconvolution” issues 1:

- Validity of modified Rician assumption: ignores polarization (see Gladysz), phasor amplitudes are not identically distributed, phasor phases are not uniformly distributed over $(-\pi, \pi)$ → Not modified Rician, and finding the correct distribution likely will be difficult

“statistical deconvolution” issues 2:

- Planetary intensity does not follow Strehl ratio if it is too close to the center, but that is the most fruitful region in the image.
- Treats data only as histogram, does not use spatio-temporal relationships between SC data (example: does not take advantage of dark speckles to constrain planetary intensity)
- However, it is worth more investigation.

Comprehensive Regression Approach:

- The major cause of difficulty is the quasi-static speckles that remain after averaging over the turbulence.
- The quasi-static speckles are caused by quasi-static aberrations in the optical system.
- I showed mathematically that the wavefront sensor data stream and millisecond exposures can be used to simultaneously determine the aberrations and the planetary image self-consistently, obviating the need for differential imaging.

The Astrophysical Journal, 767:21 (11pp), 2013 April 10 doi:10.1088/0004-637X/767/1/21

UTILIZATION OF THE WAVEFRONT SENSOR AND SHORT-EXPOSURE IMAGES FOR SIMULTANEOUS ESTIMATION OF QUASI-STATIC ABERRATION AND EXOPLANET INTENSITY

Richard A. Frazin
Department of Atmospheric, Oceanic and Space Sciences, University of Michigan, Ann Arbor, MI 48109, USA; rfrazin@umich.edu
Received 2012 November 20; accepted 2013 February 13; published 2013 March 21

ABSTRACT

Heretofore, the literature on exoplanet detection with coronagraphic telescope systems has paid little attention to the information content of short exposures and methods of utilizing the measurements of adaptive optics wavefront sensors. This paper provides a framework for the incorporation of the wavefront sensor measurements in the context of observing modes in which the science camera takes millisecond exposures. In this formulation, the wavefront sensor measurements provide a means to jointly estimate the static speckle and the planetary signal. The ability to estimate planetary intensities in as little as a few seconds has the potential to greatly improve the efficiency of exoplanet search surveys. For simplicity, the mathematical development assumes a simple optical system with an idealized Lyot coronagraph. Unlike currently used methods, in which increasing the observation time beyond a certain threshold is useless, this method produces estimates whose error covariances decrease more quickly than inversely proportional to the observation time. This is due to the fact that the estimates of the quasi-static aberrations are informed by a new random (but approximately known) wavefront every millisecond. The method can be extended to include angular (due to diurnal field rotation) and spectral diversity. Numerical experiments are performed with wavefront data from the AEOS Adaptive Optics System sensing at 850 nm. These experiments assume a science camera wavelength λ of 1.1 μ, that the measured wavefronts are exact, and a Gaussian approximation of shot-noise. The effects of detector read-out noise and other issues are left to future investigations. A number of static aberrations are introduced, including one with a spatial frequency exactly corresponding the planet location, which was at a distance of $\approx 3\lambda/D$ from the star. Using only 4 s of simulated observation time, a planetary intensity, of ≈ 1 photon ms^{-1}, and a stellar intensity of $\approx 10^5$ photons ms^{-1} (contrast ratio 10^5), the short-exposure estimation method recovers the amplitudes' static aberrations with 1% accuracy, and the planet brightness with 20% accuracy.

How does the regression approach work?

- Create ms data cubes, one for the SC measurements and another for the WFS measurements
- Make a model that connects the WFS data cube to the AO residual phase
- Make model that connects the SC data cube to the unknown parameters that describe the optical aberrations [either explicitly or, more easily, in terms of an Emprical Green's Function (EGF)] and the planetary image.
- Use statistical inference procedure.

Regression approach can include:

- Diurnal rotation constraints (used by ADI)
- Multi-wavelength constraints (used by SDI)
- Polarization constraints (used by PDI)
- Speckle cancelation strategies
- Multi-DM modulation
- Self-coherent camera information

Bayesian/EiV approach

Potential Hurdles

- Detector readout noise – New generation of NIR detectors is capable of kHz readout and about 1 e noise per pixel.
- Need precise calibration of WFS – Solve for bias and gain errors (as shown in equation)
- 1 kHz rate → 1 M images in 17 m. Huge data processing demand – Sequential estimation based on Kalman filtering
- Need models of AO residual reconstruction error
- Complicated but interesting statistical issues – Collaborate with statistician

C’est Tout